

**Effect of flux flow on microwave losses in  $\text{YBa}_2\text{Cu}_3\text{O}_{7-x}$  superconducting films**

A. G. Zaitsev, R. Schneider, G. Linker, F. Ratzel, R. Smithey, and J. Geerk

*Forschungszentrum Karlsruhe, Institut für Festkörperphysik, D-76021 Karlsruhe, Germany*

(Received 27 January 2003; revised manuscript received 15 May 2003; published 4 September 2003)

Microwave losses in  $\text{YBa}_2\text{Cu}_3\text{O}_{7-x}$  (YBCO) films carrying overcritical currents were measured at several temperatures between 74 and 85 K, and found to be in good agreement with the predictions of the vortex dynamics model for the magnetic flux flow. For the measurements a 2.3-GHz microstrip resonator made of an epitaxial double-sided YBCO film on  $\text{CeO}_2$  buffered sapphire was equipped with a Cu coil, which is usually used for ac (1.1 kHz) inductive measurements of the critical current density  $J_C$ . The ac current density induced in the film,  $J_{\text{ind}}$  controlled the vortex flow, while the microwave surface impedance ( $Z_S = R_S + iX_S$ ) of the film was measured as a function of  $J_{\text{ind}}$ . Both  $R_S$  and  $X_S$  remained fairly constant for  $J_{\text{ind}} < J_C$ , indicating a weak contribution of the thermally activated flux flow to the microwave loss. The loss revealed a sharp increase at  $J_{\text{ind}} \approx J_C$ . In the flux flow regime,  $J_{\text{ind}} \geq 2J_C$ , both  $\Delta R_S$  and  $\Delta X_S$  were linear with  $J_{\text{ind}}$ . This behavior of the microwave losses agrees well with the dependence  $\Delta Z_S = \rho_f / 2\lambda_L$  predicted by the vortex dynamics model ( $\lambda_L$  is the London penetration depth and  $\rho_f$  is the complex flux flow resistivity of type-II superconductors). The ratio  $\Delta X_S / \Delta R_S$  in the flux flow regime was independent of  $J_{\text{ind}}$  and increased with decreasing temperature from 2.7 at 85 K to 7.9 at 74 K, in agreement with the model.

DOI: 10.1103/PhysRevB.68.104502

PACS number(s): 74.78.Bz, 74.25.Nf, 74.25.Qt

The treatment of the current-voltage ( $I$ - $V$ ) characteristics of type-II superconductors in terms of the vortex dynamics belongs to the well-established physical fundamentals for both low-temperature and high-temperature superconductors (HTSCs); see Refs. 1–3 for review. It considers the dissipation resulting from the motion of the magnetic flux carried by the vortices and driven by the Lorentz force exerted on the vortices by the transport current,  $J$ . The balance between the Lorentz force and the pinning force determines the critical current density  $J_C$ . The relation between these two forces also determines the mechanism of the flux motion, which varies from the thermally activated *flux creep* at undercritical  $J$  to the *flux flow* at overcritical  $J$ . This approach was extended to microwave frequencies in order to explain the effect of the vortex motion on the hf surface impedance ( $Z_S = R_S + iX_S$ ) of type-II superconductors; for reviews, see Refs. 3–5. However, an application of the developed model for the interpretation of the microwave measurements on HTSC thin films was mostly limited to low-hf power measurements in dc magnetic fields,<sup>6–10</sup> i.e., to the case of small undercritical currents and thermally activated vortex motion. The case of the flux flow sustained by overcritical currents turned out to be difficult for experimental verification. In particular, the increase of  $Z_S$  of HTSC films with increasing hf power in zero dc fields could not be explained quantitatively in terms of the vortex dynamics model.<sup>5,11</sup> The disagreement was attributed to the effect of other hf loss mechanisms, like losses in Josephson-like grain boundaries<sup>12</sup> and weak links,<sup>13,14</sup> hysteretic losses treated within the framework of the Bean model,<sup>15,16</sup> local heating,<sup>5</sup> etc., which should overshadow the flux flow losses. But a significant deviation in the hf response of the vortices flowing in HTSC films from the basic predictions of the vortex dynamics model could not be ruled out, either.

The aim of the present work is to propose a direct experiment for measuring the hf losses in HTSC films due to vortices flowing under the influence of an overcritical transport current, and to verify the treatment of such hf losses within

the framework of the vortex dynamics model. For the measurements we used microstrip resonators prepared of double-sided  $\text{YBa}_2\text{Cu}_3\text{O}_{7-x}$  (YBCO) films. In contrast to former experiments,<sup>5,11–16</sup> we controlled the vortex motion in the films not by increasing the microwave current in the resonator, but by inducing an external ac current  $J_{\text{ind}}$  in the films, which is a technique similar to the inductive  $J_C$  measurements.<sup>17</sup> The contribution of the moving vortices to the surface resistance and surface reactance of the YBCO films was evaluated from the decrease of the quality factor of the resonator and the shift of its resonance frequency, respectively. The microwave current was kept constant and low in order to avoid its contribution to vortex depinning. The surface impedance of the films,  $Z_S$ , was measured as a function of  $J_{\text{ind}}$  which was varied from zero up to several times the critical current density  $J_C$ . This allowed us to probe different regimes of the vortex motion from the thermal activation to the flux flow.

Double-sided 400-nm-thick YBCO films on  $\text{CeO}_2$  buffered sapphire substrates were prepared using the ASIDOD technique.<sup>18</sup> In the ASIDOD system a three-inch diameter sapphire wafer is simultaneously coated on both sides by using two face-to-face inverted cylindrical sputter guns attached to a cavitylike heater. The  $\text{CeO}_2$  targets are rf sputtered, and the YBCO targets are dc sputtered. The homogeneity of the coating over large areas is attained by a rotation and linear motion of the wafer inside the heater during the sputtering. The films exhibited a high transition temperature,  $T_C = 90$ – $90.5$  K, and good superconducting and microwave properties, which were reported in detail elsewhere<sup>18–20</sup> together with details of the patterning and contacting processes. Microstrip half-wavelength resonators were prepared using the hairpinlike layout shown in Fig. 1. The width of the microstrip lines of 0.41 mm corresponded to the 50- $\Omega$  wave impedance on the 0.43-mm-thick sapphire substrate. The distance between the hairpin lines was 0.3 mm. The length of the resonator of 27.2 mm yielded a fundamental frequency of  $f_0 \approx 2.3$  GHz. The geometry factor of the resonator,  $G$

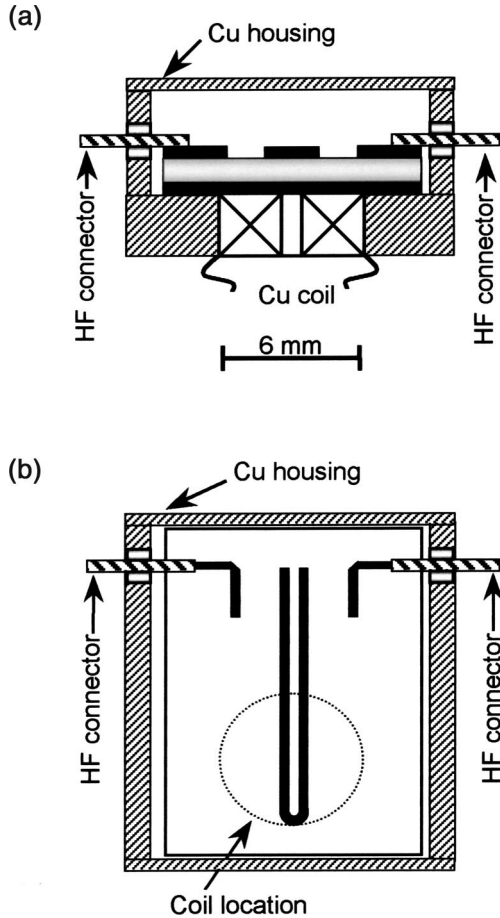


FIG. 1. Schematic arrangement of the measurement system: (a) cross section, (b) top view.

$=1.81 \Omega$ , was calculated using Sonnet software,<sup>21</sup> which automatically took into account the coupling between the two lines of the hairpin. The resonator was fixed in a Cu housing, as shown in Fig. 1. At the bottom of the housing a Cu coil of 6-mm diameter was mounted under the hairpin's bending; see Fig. 1. It is known that the sinelike hf current distribution along a half-wavelength resonator is maximal at the center and almost zero at the ends of the resonator line.<sup>22</sup> Thus, the coil was capable to induce the ac currents in the resonator area, which carried the maximum hf currents. Initially such coils were developed for inductive  $J_C$  measurements.<sup>23</sup> They had two windings of a 50- $\mu\text{m}$ -thick wire: a driving one with 1100 turns and a pickup one with 110 turns. The driving winding operating at 1.1 kHz was capable of producing a magnetic field of up to several 100 Oe at the film surface. This was enough to induce current densities  $J_{\text{ind}}$  of up to  $\sim 8 \text{ MA/cm}^2$  in the YBCO film, whereas the onset of the third harmonic signal in the pickup winding indicated that the  $J_C$  of the film was reached. The measurements at higher  $J_{\text{ind}}$  were hampered by the coil heating, which limited the measurement range to moderate  $J_C$  values, i.e., to temperatures not too far below  $T_C$ . For our YBCO films  $J_C$  measurements down to temperatures of  $\sim 60 \text{ K}$  were possible.

The microwave measurements on the resonators were performed using an HP8720C network analyzer. At low hf input power ( $P_{\text{in}} < -5 \text{ dBm}$ ) and  $J_{\text{ind}} = 0$  the resonator perfor-

mance was linear, with both the quality factor and the resonance frequency independent of the hf power. Under these conditions the "linear" microwave surface resistance of the YBCO films was determined as  $R_S = G/Q_0$ , where  $Q_0$  is its unloaded quality factor. The absolute values of the microwave surface reactance,  $X_S$ , were estimated from our measurements of the absolute London penetration depth,  $\lambda_L$ , in the YBCO films on sapphire.<sup>20</sup> Here the standard relation  $X_S = \omega_0 \mu_0 \lambda_L$  was used, with  $\omega_0$  the circular resonance frequency and  $\mu_0 = 4\pi \times 10^{-7} \text{ H/m}$  the magnetic permeability of the vacuum.

An increase of  $J_{\text{ind}}$  led to a decrease of both  $Q_0$  and  $\omega_0$ . The change of these quantities was transformed into a change of the microwave surface impedance using the standard formula<sup>4,5</sup>

$$\Delta Z_S = \Delta R_S + i\Delta X_S = G\Delta(Q_0^{-1}) + i2G(\Delta\omega_0/\omega_0). \quad (1)$$

In this way  $\Delta R_S$  and  $\Delta X_S$ , and their ratio  $\Delta X_S/\Delta R_S$ , were measured as a function of  $J_{\text{ind}}$  at various temperatures between 85 and 74 K. Below 74 K  $J_C$  of the films became too high for our measurement apparatus, so that a sufficient excess of  $J_{\text{ind}}$  over  $J_C$  could not be supplied. Typical examples of the obtained curves are displayed in Fig. 2. For the sake of easier comparison the data are plotted versus  $J_{\text{ind}}/J_C$ . The temperature dependences of  $R_S$ ,  $X_S$ , and  $J_C$  are shown in the insets of Fig. 2 as a reference.

The obtained dependences of  $\Delta R_S$  and  $\Delta X_S$  vs  $J_{\text{ind}}/J_C$  reproduce the well-known shape of  $I$ - $V$  characteristics in type-II superconductors. There is a clear turning point in these dependences at  $J_{\text{ind}}/J_C = 1$ . Below this point the pinning force prevails over the Lorentz force, the vortex motion occurs only due to thermal fluctuations and the losses are relatively low. In our experiment for  $J_{\text{ind}}/J_C < 1$  both,  $\Delta R_S$  and  $\Delta X_S$ , remained under the resolution limit of  $\sim 1 \mu\Omega$ . Consequently, their ratio  $\Delta X_S/\Delta R_S$  could not be defined. The onset in  $\Delta R_S$  and  $\Delta X_S$  appeared at  $J_{\text{ind}}/J_C \approx 1$ , and was characterized by relatively high  $\Delta X_S/\Delta R_S$  values of 30–50; see Fig. 2(c). A further increase of  $J_{\text{ind}}/J_C$  resulted in a rapid increase of both  $\Delta X_S$  and  $\Delta R_S$  and a decrease of their ratio to values of about 3–10 depending on the measurement temperature. At  $J_{\text{ind}}/J_C > 2$  both  $\Delta X_S$  and  $\Delta R_S$  grew linearly with  $J_{\text{ind}}/J_C$ , while their ratio  $r$  was  $J_{\text{ind}}$  independent.

The analysis of the experimental data was performed in terms of the vortex dynamics model. The application of this model for predicting hf losses in type-II superconductors in the mixed state has been subject of many publications,<sup>3–5</sup> that developed an extensive formalism usually accomplished by considering various approximations in high and low field and frequency limits. Therefore, we found it reasonable to review the established basics of the model and to obtain concise relations directly applicable for the evaluation of our experimental results.

The core mechanism in the model is the interaction between the harmonic sinusoidal hf electric current and the vortices, each carrying a magnetic flux quantum  $\Phi_0$ . If the vortices are able to follow the resulting Lorentz force, they start moving, or vibrating, with the hf frequency. Such a motion of the magnetic flux induces a hf electric field oppos-

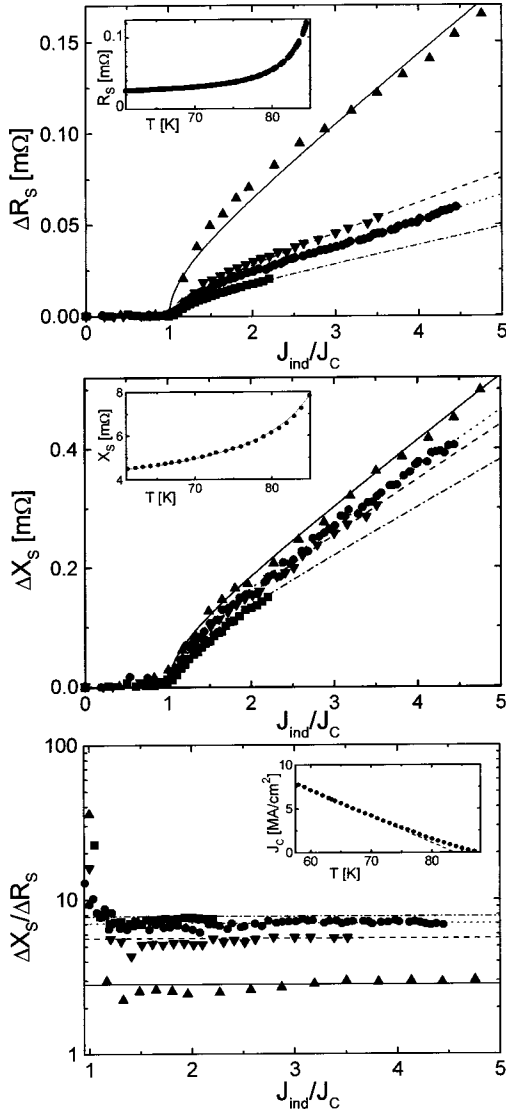


FIG. 2. Dependences of  $\Delta R_S$  (a), and  $\Delta X_S$  (b), and their ratio  $\Delta X_S/\Delta R_S$  (c), on the  $J_{\text{ind}}/J_C$  ratio measured at the following temperatures: (▲), 85.1 K; (▼), 79 K; (●), 77.4 K; and (■), 74 K. The lines show the best fits of Eqs. (9) and (10) to the experimental data: solid lines 85.1 K; dotted lines 79 K; dashed lines 77.4 K; and dot-dashed line 74 K. Measured temperature dependences of  $R_S$  and  $J_C$  are shown in the insets of (a) and (c), respectively. The inset of (b) shows the  $X_S(T)$  data obtained from the  $\lambda_L$  measurements on our double-sided YBCO films on buffered sapphire (Ref. 20).

ing the hf current. Consequently, a complex electric resistivity  $\rho_f$  arises, that is called the flux flow resistivity. The real part of  $\rho_f$  is controlled by the viscous drag force, whereas its imaginary part is controlled by the vortex elasticity and inertia. Considering the related equation of motion and neglecting the inertia at frequencies below  $\sim 100$  GHz, the model yields<sup>5</sup>

$$\rho_f = \frac{\Phi_0^2 n_f}{\eta(1+r^2)}(1+ir), \quad (2)$$

with  $r = \chi/\omega\eta$ . Here  $n_f$  is the density of the moving vortices,  $\eta$  is the vortex viscosity,  $\chi$  is the vortex restoring force con-

stant, often named the pinning constant, and  $\omega$  is the radial frequency of the hf current. One may see that Eq. (2) is valid only at nonzero frequencies. In fact,  $\omega/2\pi$  should be higher than the reciprocal value of the vortex relaxation time  $1/\tau$ , which is well fulfilled at microwave frequencies.<sup>3,5</sup> The ratio  $\chi/\eta$  represents a crossover frequency  $\omega_c$ , discriminating between low frequencies,  $\omega < \omega_c$ , at which the flux motion is mainly reactive ( $\text{Im}\rho_f > \text{Re}\rho_f$ ), and high frequencies,  $\omega > \omega_c$ , at which the flux motion is mainly dissipative ( $\text{Re}\rho_f > \text{Im}\rho_f$ ). In the literature  $\omega_c$  is often called a “depinning” or “pinning” frequency.

Taking  $\rho_f$  into account, one accomplishes the conventional two-fluid model for the superconductors by rewriting Ohm’s law as follows:

$$J_{\text{HF}} = \sigma_{\text{TF}}(E_{\text{HF}} - \rho_f J_{\text{HF}}) = \frac{\sigma_{\text{TF}}}{1 + \sigma_{\text{TF}}\rho_f} E_{\text{HF}} = \sigma_{\text{MS}} E_{\text{HF}}, \quad (3)$$

where  $J_{\text{HF}}$  is the hf current density,  $E_{\text{HF}}$  is the related electric field,  $\sigma_{\text{TF}} = \sigma_N - i/(\omega\mu_0\lambda_L^2)$  is the complex conductivity of a superconductor without vortex motion,  $\sigma_N$  is the normal fluid conductivity, and  $\sigma_{\text{MS}} = \sigma_{\text{TF}}/(1 + \sigma_{\text{TF}}\rho_f)$  represents the complex conductivity in the mixed state.

Equation (3) leads to a general expression for the hf surface impedance of type-II superconductors in the mixed state:

$$Z_{\text{MS}} = \left( \frac{i\omega\mu_0}{\sigma_{\text{MS}}} \right)^{1/2} = Z_S \sqrt{1 + \sigma_{\text{TF}}\rho_f} \quad (4)$$

where  $Z_S = \sqrt{i\omega\mu_0/\sigma_{\text{TF}}}$  is the conventional relation for the hf surface impedance in terms of the two-fluid model.

Within the framework of the two-fluid model  $\lambda_L^2\omega\mu_0\sigma_N \ll 1$ , which means that the superconducting fluid carries much higher hf current than the normal one, and makes  $R_S \ll X_S$ .<sup>4,5</sup> This approximation allows us to combine the relations for  $\sigma_{\text{TF}}$  and  $\rho_f$  into the following one:

$$\sigma_{\text{TF}}\rho_f = \frac{-i\rho_f}{\lambda_L^2\omega\mu_0} = \frac{-i\rho_f}{\lambda_L X_S}. \quad (5)$$

Here we limit our treatment to the case of a weak nonlinearity, i.e.,  $\sigma_{\text{TF}}\rho_f \ll 1$ , and express Eq. (4) as  $Z_{\text{MS}} \approx Z_S(1 + \sigma_{\text{TF}}\rho_f/2)$ . Again using  $R_S \ll X_S$ , we obtain a compact general relation for the excess hf losses produced in a type-II superconductor by the moving vortices:

$$\Delta Z_S = Z_{\text{MS}} - Z_S = \frac{\rho_f}{2\lambda_L}. \quad (6)$$

Substituting Eq. (2) into Eq. (6) we obtain the well-known relations, which are usually derived applying a more complicated formalism:<sup>4,5</sup>

$$\Delta R_S = \frac{\Phi_0^2 n_f}{2\lambda_L \eta(1+r^2)},$$

$$\Delta X_S = \frac{\Phi_0^2 n_f}{2\lambda_L \eta(1+r^2)} r \quad \text{and} \quad \frac{\Delta X_S}{\Delta R_S} = r. \quad (7)$$

Quantitatively, the vortex dynamics model for YBCO predicts  $r \gg 1$ , or somewhat higher, which agrees with the results of hf measurements in applied dc magnetic fields.<sup>5,8,9,24</sup>

Using Eqs. (5)–(7) we specify the criterion for the weak non-linearities as follows: The condition  $\sigma_{\text{TF}}\rho_f \ll 1$  is satisfied, if both,  $\Delta R_S$  and  $\Delta X_S$ , are small compared to  $X_S$ . The relation of  $\Delta R_S$  and  $\Delta X_S$  to  $R_S$  is not decisive. In our measurements the YBCO films exhibited  $X_S$  values of several m $\Omega$ , which is much higher than the observed  $\Delta X_S$  and  $\Delta R_S$ ; see Fig. 2. Thus, we consider the measured nonlinearities as weak and apply Eqs. (6) and (7) for their analysis.

In our experiment the density of the moving vortices is controlled by the induced current  $J_{\text{ind}}$ . For  $J_{\text{ind}} > J_C$  it is expected to behave like<sup>3</sup>

$$n_f \propto (1 - J_c^2/J_{\text{ind}}^2)^{1/2} H, \quad (8)$$

where  $H$  is the amplitude of the ac magnetic field at the YBCO film surface, which is directly proportional to  $J_{\text{ind}}$ . According to Eq. (7)  $\Delta R_S$  and  $\Delta X_S$  exhibit a linear dependence on  $n_f$ , provided the vortex parameters  $\eta$  and  $\chi$  remain constant. Thus, we obtain the following fitting relations for the measured hf losses in the flux flow regime:

$$\Delta R_S = c_1(T) (J_{\text{ind}}^2/J_c^2 - 1)^{1/2} \quad (9)$$

$$\Delta X_S = c_2(T) (J_{\text{ind}}^2/J_c^2 - 1)^{1/2}, \quad (10)$$

where  $c_1(T)$  and  $c_2(T)$  are the fitting parameters, dependent on temperature and independent of  $J_{\text{ind}}$ . The ratio  $c_2(T)/c_1(T)$  should fit the measured  $\Delta X_S/\Delta R_S$  data at a given temperature.

One may notice that Eqs. (9) and (10) are directly applicable only for a dc  $J_{\text{ind}}$ . For an ac  $J_{\text{ind}}$ , which is the case in the present experiment, the losses in the resonator should be modulated with the ac frequency. Indeed, using a spectrum analyzer we observed this expected mixing of the hf (2.3 GHz) and the ac (1.1 kHz) frequencies at  $J_{\text{ind}} > J_C$ . However, since the  $\Delta X_S$  and  $\Delta R_S$  values obtained in the present experiment are time averaged, we do not focus more closely on the frequency mixing, and consider Eqs. (9) and (10) as valid for the rms values. The difference between the dc to the rms values in Eqs. (9) and (10) should be encountered in the constants  $c_1$  and  $c_2$ . However, we are not interested in the absolute values of these constants. Our further interest is mostly devoted to their ratio,  $c_2/c_1$ , which is not affected by averaging.

It is shown in Fig. 2, that the measured dependences of  $\Delta X_S$  and  $\Delta R_S$  on  $J_{\text{ind}}/J_C$  behave in good agreement with Eqs. (9) and (10) for  $J_{\text{ind}}/J_C \gg 1.1$ , indicating that the flux flow is responsible for the observed excess hf loss. In the small range of  $1 < J_{\text{ind}}/J_C < 1.1$  the high  $\Delta X_S/\Delta R_S$  values of 30–50 suggest an additional effect of another hf loss mechanism,<sup>5,24</sup> probably losses in weakly coupled grains, which compete with the flux flow effect. The rise of  $J_{\text{ind}}/J_C$  above 1.1 and the enhancement of the flux flow increase substantially the density of the moving vortices in the YBCO film; see Eq. (7). This results in a rapid increase of both  $\Delta X_S$  and  $\Delta R_S$  and a decrease of their ratio to the values of about 3–10 consistent with the vortex dynamics model.<sup>5,24</sup> In par-

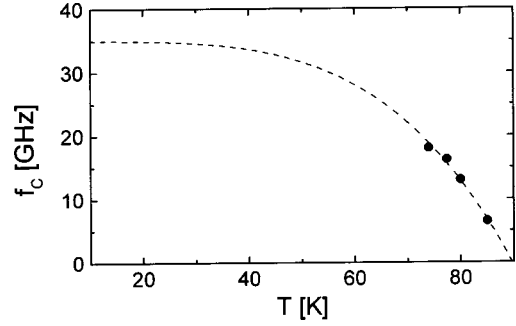


FIG. 3. Temperature dependence of the crossover frequency. The circles mark the experimental data, the dashed curve is calculated using Eq. (14) and  $f_c(0) = 35$  GHz as a fitting parameter.

ticular, a good fit of Eqs. (9) and (10) to the experimental data implies, that the vortex parameters  $\eta$  and  $\chi$  do not depend on  $J_{\text{ind}}$ , i.e., they are independent of the magnetic field and the depinning current density.

The ratio  $\Delta X_S/\Delta R_S$  provides, according to Eq. (7), a direct measure of the crossover frequency, one of the key parameters in the vortex dynamics model, which is defined on the basis of Eq. (2):

$$f_c = \frac{\Delta X_S}{\Delta R_S} f_0. \quad (11)$$

The obtained  $f_c$  values are plotted in Fig. 3. They increase with decreasing temperature from 6.5 GHz at 85.1 K to 18 GHz at 74 K. Comparing these data with results of microwave measurements in dc magnetic fields,<sup>6–10</sup> one should take into account a considerable scatter in the  $f_c(T)$  data reported by different groups, which likely results from the high sensitivity of the vortex parameters to sample quality. In particular,  $f_c$  increasing from 3 GHz at 85 K to 15 GHz at 80 K was reported by Owliaei *et al.*<sup>6</sup> Golosovsky *et al.*<sup>8</sup> reported  $f_c$  values increasing from 4 to 6 GHz at temperatures decreasing from 85 to 70 K. These results provide a broad reference range of absolute  $f_c$  values, which is met by our data.

Regarding the  $f_c(T)$  dependence, we found our data in good agreement with the basic predictions of the vortex dynamics model. In particular, the Bardeen-Stephen expression is usually accepted as a good approximation for the vortex viscosity,<sup>5–8</sup>

$$\eta = \Phi_0 H_{c2} \sigma_N, \quad (12)$$

where  $H_{c2}$  is the upper critical field. In accordance with Eq. (12) the vortex viscosity does not depend on the amplitude of the applied magnetic field, which is in agreement with our results. The related temperature dependence is given by  $\eta(t) = \eta(0)(1 - t^2)/(1 + t^2)$ , where  $t = T/T_C$  is the reduced temperature. According to the literature, the effect of the field and temperature on the vortex pinning constant  $\chi$  should be determined by the range of the applied magnetic field.<sup>4–9,25</sup> In the low-field range ( $\mu_0 H \ll 1$  T), which is the case for our measurements,  $\chi$  is expected to be proportional to the square of the thermodynamic critical field:<sup>9,25</sup>

$$\chi = \pi B_c^2 / \mu_0. \quad (13)$$

Equation (13) predicts a field-independent  $\chi$ , which is in agreement with our findings. The temperature dependence resulting from Eq. (13) is  $\chi(t) = \chi(0) \cdot (1 - t^2)^2$ . Consequently, for the crossover frequency one obtains

$$f_c(T) = f_c(0) [1 - (T/T_c)^4], \quad (14)$$

where  $f_c(0) = \chi(0) / 2\pi\eta(0)$ . Equation (14) predicts a strongly decreasing  $f_c(T)$  in the higher temperature range, which agrees well with our experimental results; see Fig. 3. Using Eq. (14) we extrapolated our  $f_c(T)$  data to lower temperatures and obtained  $f_c(0) = 35$  GHz. This value is in reasonable agreement with the data of Ref. 7, which estimated  $f_c$  to be somewhat higher than 40 GHz at  $T < 40$  K for epitaxial YBCO films.

In summary, we have measured the microwave losses produced in epitaxial YBCO films by the vortices flowing under the influence of overcritical currents. The results were found to be in good agreement with the vortex dynamics model. The observed behavior of the microwave losses is adequately described by the relation  $\Delta Z_S = \rho_f / 2\lambda_L$ , derived in terms of the model. The vortex viscosity and restoring force constants, which determine the  $\rho_f$  value under given conditions, were confirmed to be independent of the magnetic field and the depinning current density. The temperature dependence of the vortex constants in the examined range between 74 and 85 K is characterized by a strong increase of their ratio, the crossover frequency, with decreasing temperature. This result is also in agreement with the model. The measured  $f_c$  values and the  $f_c(0)$  value obtained by extrapolating the measurement results to zero temperature agree reasonably well with the results of the hf measurements in the applied dc magnetic fields available in the literature.

<sup>1</sup>A.M. Campbell and J.E. Evetts, *Critical Currents in Superconductors* (Taylor & Francis, London, 1972).

<sup>2</sup>M.N. Kunchur, *Mod. Phys. Lett. A* **9**, 399 (1995).

<sup>3</sup>E.H. Brandt, *Physica C* **195**, 1 (1992).

<sup>4</sup>M.J. Lancaster, *Passive Microwave Device Applications of High-Temperature Superconductors* (Cambridge University Press, Cambridge, 1997), Chap. 3.

<sup>5</sup>M. Hein, *High-Temperature-Superconductor Thin Films at Microwave Frequencies*, Springer Tracts in Modern Physics Vol. 155 (Springer, Berlin, 1999), Chap. 3.

<sup>6</sup>J. Owliaei, S. Sridar, and J. Talvacchio, *Phys. Rev. Lett.* **69**, 3366 (1992).

<sup>7</sup>N. Belk, D.E. Oates, D.A. Feld, G. Dresselhaus, and M.S. Dresselhaus, *Phys. Rev. B* **53**, 3459 (1996).

<sup>8</sup>M. Golosovsky, M. Tsindlekht, H. Chayet, and D. Davidov, *Phys. Rev. B* **50**, 470 (1994).

<sup>9</sup>I. Ghosh, L.F. Cohen, and J. Gallop, *Supercond. Sci. Technol.* **10**, 936 (1997).

<sup>10</sup>J.R. Powell, A. Porch, R.G. Humphreys, F. Wellhöfer, M.J. Lancaster, and C.E. Gough, *Phys. Rev. B* **57**, 5474 (1998).

<sup>11</sup>D.E. Oates, M.A. Hein, P.J. Hirst, R.G. Humphreys, G. Koren, and E. Polturak, *Physica C* **372–376**, 462 (2002).

<sup>12</sup>H. Xin, D.E. Oates, G. Dresselhaus, and M.S. Dresselhaus, *J. Supercond.* **14**, 637 (2001).

<sup>13</sup>A.V. Velichko and A. Porch, *Phys. Rev. B* **63**, 094512 (2001).

<sup>14</sup>E. Gaganidze, R. Heidinger, J. Halbritter, and H. Schneidewind, *J. Phys. C* **372–376**, 511 (2002).

<sup>15</sup>S. Sridar, *Appl. Phys. Lett.* **65**, 1054 (1994).

<sup>16</sup>P.P. Nguyen, D.E. Oates, G. Dresselhaus, M.S. Dresselhaus, and A.C. Anderson, *Phys. Rev. B* **51**, 6686 (1995).

<sup>17</sup>J.H. Claassen, M.E. Reeves, and R.J. Soulen, Jr., *Rev. Sci. Instrum.* **62**, 996 (1991).

<sup>18</sup>J. Geerk, A. Zaitsev, G. Linker, R. Aidam, R. Schneider, F. Ratzel, R. Fromknecht, B. Scheerer, H. Reiner, E. Gaganidze, and R. Schwab, *IEEE Trans. Appl. Supercond.* **11**, 3856 (2001).

<sup>19</sup>A.G. Zaitsev, R. Schneider, G. Linker, F. Ratzel, R. Smithey, and J. Geerk, *Appl. Phys. Lett.* **79**, 4174 (2001).

<sup>20</sup>A.G. Zaitsev, R. Schneider, G. Linker, F. Ratzel, R. Smithey, and J. Geerk, *Rev. Sci. Instrum.* **73**, 335 (2002).

<sup>21</sup>Sonnet *em* high frequency electromagnetic analysis software, version 7.0b, Sonnet Software Inc.

<sup>22</sup>O.G. Vendik, I.B. Vendik, and T.B. Samoilova, *IEEE Trans. Microwave Theory Tech.* **45**, 173 (1997).

<sup>23</sup>A.G. Zaitsev, R. Schneider, J. Geerk, G. Linker, F. Ratzel, R. Smithey, S. Kolesov, and T. Kaiser, in *Characterisation of the superconducting and microwave properties of YBCO films simultaneously sputtered on both sides of sapphire wafers*, Proceedings of the European Conference on Applied Supercond., Sitges, Spain, 11–14 Sept. 1999, IOP Conf. Proc. No. 167 (IOP, Bristol, 2000), p. 307.

<sup>24</sup>M.A. Golosovsky, H.J. Snortland, and M.R. Beasley, *Phys. Rev. B* **51**, 6462 (1995).

<sup>25</sup>A.F. Hebard, P.L. Gammel, C.E. Rice, and A.F.J. Levi, *Phys. Rev. B* **40**, 5243 (1989).